# Interpretation of the Wigner Transform

M. Casas

Departament de Física, Universitat de les Illes Balears

E-07071, Palma de Mallorca, Spain

H. Krivine

Division de Physique Théorique *, Institut de Physique Nucléaire,

91406, Orsay Cedex, France

J. Martorell

Departament d'Estructura i Constituents de la Materia

Facultat de Física , Universitat de Barcelona

E-08028, Barcelona, Spain

IPNO/TH 90-01

*Unité de Recherche des Universités Paris 11 et Paris 6 Associée au C.N.R.S.

Abstract

In quantum mechanics it is not possible to define a probability for finding a particle at position $\vec{r}$ with momentum $\vec{p}$. Nevertheless there is a function introduced by Wigner, which retains many significant features of the classical probability distribution. Using simple one dimensional models we try to understand the very involved structure of this function.



Fig. 1

## I Introduction

The Heisenberg's uncertainty relations imply the impossibility to simultaneously measure with infinite accuracy the position and momentum of a particle in quantum mechanics. Therefore there is no quantal equivalent to the classical distribution function of statistical mechanics $f_{cl}(\vec{r}_1,...,\vec{r}_N,\vec{p}_1,...,\vec{p}_N)$, which defines for an ensemble of N identical particles ( in our case fermions ) the probability of finding them at the points : $\vec{r}_1,...,\vec{r}_N$, with momenta $\vec{p}_1,...,\vec{p}_N$. Many years ago Wigner [1] introduced however a quantal quantity which has many of the properties of the classical distribution function and which in the appropriate limit coincides with it. This quantal distribution function is usually called the Wigner transform and rigorous formulations of quantum mechanics ( Weyl [2] ) are based on the use of the correspondence principle to connect this quantal distribution function to the classical one. The Wigner transform is also a useful starting point to derive semiclassical approximations for the many body problem, such as Thomas Fermi, as was already shown by Wigner [1] and Kirkwood [3]. More recently, it has been also widely used by the theoreticians to study a variety of quantum processes, e.g.: in the description of the dynamics of heavy ion nuclear reactions and in atomic and molecular collisions [4], and also in the description of coherent states [5].

On a more practical level, and although the Wigner transform is not a measurable quantity, in recent years a lot of progress has been made in the experimental determination of quantities directly related to it, like mass and momentum distributions, in systems ranging from condensed matter to nuclear and quark physics. In most cases however one is not interested in the quantal equivalent of the full distribution function , but only on an integrated form of it giving the probability for finding a particle at position $\vec{r}$ with momentum $\vec{p}$, with ali the other particles positions and momenta undetermined. For these purposes it can be expected that the mean field approximation gives a sufficiently good description of the ground state of the N-fermion system , so that the interactions between the particles can be well approximated by a one body potential. The reduced Wigner transforms computed with these models show considerable structure and differ considerably

from the predictions of the simpler Thomas Fermi approximation . What we will show here is that these structures can be interpreted using elementary classical and semiclassical ideas and that this allows to recognize even in these involved quantal functions many of the signatures of the classical probability distribution for finding a particle with momentum $\vec{p}$ at position $\vec{r}$.

## II Wigner Transform

Ignoring spin and other possible intrinsic degrees of freedom, the full Wigner transform is defined as the Fourier transform of the density matrix:

$$f_W(\vec{r}_1,...,\vec{r}_N,\vec{p}_1,...,\vec{p}_N) = \int ... \int d\vec{s}_1...d\vec{s}_N \psi^*(\vec{r}_1+\frac{\vec{s}_1}{2},...,\vec{r}_N+\frac{\vec{s}_N}{2}) e^{\frac{i}{\hbar}(\vec{p}_1.\vec{s}_1+...+\vec{p}_N.\vec{s}_N)} \psi(\vec{r}_1-\frac{\vec{s}_1}{2},...,\vec{r}_N-\frac{\vec{s}_N}{2}) \quad (1)$$

and it can be easily checked that it has the following properties :

$$\frac{1}{(2\pi\hbar)^{3N}} \int f_W(\vec{r}_1,...,\vec{r}_N,\vec{p}_1,...,\vec{p}_N) d\vec{p}_1...d\vec{p}_N = |\psi(\vec{r}_1,...,\vec{r}_N)|^2 \quad (2)$$

which gives the probability for finding the particles at the points $\vec{r}_1,...,\vec{r}_N$ (with any values of their momenta), and

$$\frac{1}{(2\pi\hbar)^{3N}} \int f_W(\vec{r}_1,...,\vec{r}_N,\vec{p}_1,...,\vec{p}_N) d\vec{r}_1...d\vec{r}_N = |\tilde{\psi}(\vec{p}_1,...,\vec{p}_N)|^2 \quad (3)$$

where $\tilde{\psi}$ is the Fourier transform of $\psi$, and which gives now the probability for finding the particles with momenta $\vec{p}_1,...,\vec{p}_N$. It is also immediate to realize that the Wigner transform allows one to compute the expectation values of any operator H that depends only on positions and momenta:

$$< H >= \int H(\vec{r}_1,...,\vec{r}_N,\vec{p}_1,...,\vec{p}_N) f_W(\vec{r}_1,...,\vec{r}_N,\vec{p}_1,...,\vec{p}_N) d\vec{r}_1...d\vec{r}_N d\vec{p}_1...d\vec{p}_N \quad (4)$$

Since the classical distribution function, $f_{cl}(\vec{r}_1,...,\vec{r}_N,\vec{p}_1,...,\vec{p}_N)$, has the same properties this leads to the interpretation of Wigner's transform as its quantal analog . However,

important differences remain : in particular, it is easy to check with simple examples ( some will be explicitly shown later ) that $f_W(\vec{r},\vec{p})$ is not positive definite and therefore cannot be a probability density.

The reduced Wigner transform is defined as :

$$f(\vec{r},\vec{p}) = \int ... \int d\vec{r}_2 ... d\vec{r}_N d\vec{p}_2 ... d\vec{p}_N f_W(\vec{r},\vec{r}_2,...,\vec{r}_N,\vec{p},\vec{p}_2,...,\vec{p}_N) \tag{5}$$

And , in particular, for a system of N fermions described by a Slater determinant of single particle wavefunctions $\{\phi_i(\vec{r}), i = 1,....,N\}$ , is given by

$$f(\vec{r},\vec{p}) = \sum_{i=1}^{N} \int \phi_i^*(\vec{r}_1 + \frac{\vec{s}}{2}) \phi_i(\vec{r}_2 - \frac{\vec{s}}{2}) e^{\frac{i\vec{p}.\vec{s}}{\hbar}} \, d\vec{s}. \tag{6}$$

Hence

$$\frac{1}{(2\pi\hbar)^3} \int f(\vec{r},\vec{p}) \, d\vec{p} = \rho(\vec{r}) = \sum_{i=1}^{N} |\phi_i(\vec{r})|^2 \tag{7}$$

where $\rho(\vec{r})$ is the total density in $\vec{r}$-space,i.e.: the probability for finding a particle at point $\vec{r}$ with any value of its momentum. Similarly, the total density in momentum space is given by :

$$\frac{1}{(2\pi\hbar)^3} \int f(\vec{r},\vec{p}) \, d\vec{r} = \rho(\vec{p}) = \sum_{i=1}^{N} |\tilde{\phi}_i(\vec{p})|^2 \tag{8}$$

where $\tilde{\phi}_i(\vec{p})$ is the Fourier transform of $\phi_i(\vec{r})$ .

Even this reduced Wigner transform is rather cumbersome to compute for realistic cases [15-6-7]. We show in Fig. 1 a calculation for the ground state of the atomic nucleus $^{40}Ca$ (N=Z=20). We assume that the nucleons are confined by the Woods Saxon potential [8]:

$$V(r) = \frac{V_0}{1 + e^{\frac{r - R_0}{a_0}}} \tag{9}$$

We solve numerically the Schrodinger equation and using (6) we obtain the Wigner transform. When the potential is spherically symmetric it can be shown [7 and refs. therein] that $f$ depends only on the moduli of $r$ and $p$ and on the angle between them. This latter dependence is very weak for closed shell systems [7] and therefore what is shown is an



Fig. 3

angle averaged Wigner transform. It should be noticed that more realistic calculations using Hartree Fock wavefunctions [7] give Wigner transforms that are undistinguishable from the one above when plotted on the scale of Fig. 1. In the same figure is also shown the distribution function predicted by the Thomas Fermi model :

$$f_{TF}(\vec{r},\vec{p}) = 4\theta(E - H_{cl}) \tag{10}$$

where $H_{cl}$ is the classical hamiltonian given by $H_{cl} = V(r) + \frac{p^2}{2m}$. $E$ is the Fermi energy obtained by requiring that $f_{TF}$ when integrated over $\vec{r}$ and $\vec{p}$ gives the chosen number of nucleons. The factor 4 accounts for spin and isospin degeneracy. It is seen that $f_{TF}(\vec{r},\vec{p})$ only predicts the gross features of the Wigner transfom, i.e.: its volume in phase space. The strong peak at $p = r = 0$ gives however little contributions to integrals like that in eq.(7) or (8) : in spherical coordinates $d\vec{r} = r^2 d\Omega$ and the extra $r^2$ factor suppresses the peak close to the origin. The strong oscillatory behaviour is a characteristic quantal effect that goes beyond the Thomas Fermi approximation. What we want to show in the following is that these oscillations can be interpreted using very simple ( and classical ) ideas, and that the analogy between classical and quantal transforms goes much further than the mere Thomas Fermi approximation. For simplicity we will deal only with one dimensional systems, beginning with one particle and going from this simple case to more involved ones. This is not a merely academic case : see for instance the analysis of time frequency distribution for electromagnetic waves [14].

## III One Dimensional Systems

### a) One particle

We begin with a single plane wave:

$$\phi_{p.w.}(x) = \frac{1}{\sqrt{2\pi}} e^{-ikx} \tag{11}$$

whose Wigner transform is:

$$f_{p.w.}(q,p) = \delta(\frac{p}{\hbar} - k) \tag{12}$$

Next we consider the superposition of two plane waves with equal and opposite momenta:

$$\phi_{2p.w.}(x) = Nsinkx \tag{13}$$

, and for simplicity we fix the normalization setting N=1. Then

$$f_{2p.w.}(q,p) = \frac{\pi}{2}(\delta(\frac{p}{\hbar} - k) + \delta(\frac{p}{\hbar} + k) - 2cos(2kq)\delta(\frac{p}{\hbar})) \tag{14}$$

If the superposition is due to reflection on an infinite wall at x= 0

$$\phi_r(x) = sinkx\theta(x), \tag{15}$$

where $\theta$ is the Heaviside function. The Wigner transform is

$$f_r(q,p) = q(j_0(2q(\frac{p}{\hbar} - k)) + j_0(2q(\frac{p}{\hbar} + k)) - 2cos(2qk)j_0(2q\frac{p}{\hbar}))\theta(q) \tag{16}$$

It is seen that $f_{p.w.}(q,p)$ has precisely the form that one would expect from the classical analogy : a state with well defined momentum, $\hbar k$, and which is just the delta function in eq.(12). Similarly it is easy to check that for a state with well defined position, $x$, the Wigner transform is just $\delta(q-x)$ .The next example, $\phi_{2p.w.}$, shows that superposing two plane waves gives again something that has a classical analog: the delta functions at $p = \pm\hbar k$ , but also an additional term due to genuine interferences : is has zero width in momentum, at p=0, and oscillates in $q$ with wavelength $\lambda = \pi/k$. This a characteristic quantal signature without classical analog. It will be apparent later that a term of this kind is always present in all the Wigner transforms of bound orbitals. The reflecting potential considered in the third example has an additional effect not present in the previous cases: the particle is confined to the right of the wall and due to this what are being superposed are no more states with well defined momenta, $\pm\hbar k$. This shows up in $f_r$ in the replacement of the delta distribution by spherical Bessel functions. (It is easy to show from eq.(16) that one recovers eq (14) when $q \to \infty$). These are still peaked at the classical values of the momenta, but now the distribution is broadened in momentum. A simple estimate of the width, $\Delta p$, of the peaks is given by the distance between the maximum and the first zero of the Bessel function (Rayleigh criterium). For the three peaks the result is the same :

$$\Delta p = \frac{\hbar\pi}{2q} \tag{17}$$

In addition the height of these peaks is finite. It is now:

$$f_{r,max} = q(1 - j_0(\frac{4pq}{\hbar}))\theta(q) \tag{18}$$

Eqs. (17) and (18) show that at q=0 the effect of the wall is maximal: the peaks disappear both because their height vanishes and because their width tends to infinity. However, going away from the wall the classical image recovers its validity. Thinking in classical terms (no interferences) one would expect that since in $\phi_r$ the flux of incoming particles ( and that of reflected ones ) is independent of $x$, the probability to find one of these at a given point, as given by $f_r$, should also be independent of $q$. Measuring that probability by the $f_{r,max}$ given in (18) this appears not to be so. However a better estimate of the flux of incoming particles has to take into account the broadening of the peak. To do this in the simplest way we take the product $\Delta p.f_{r,max}$ and then indeed recover $\frac{\hbar}{4}(1 - j_0(\frac{4qp}{\hbar}))$ which becomes $q$- independent far away from the wall.

We consider now the infinite square well potential. A bound state in this potential can be viewed as a standing wave i.e.: a plane wave bouncing back and forth from each wall, with a wavelength fixed by the requirement of vanishing at the boundary. Its normalized wave function can be written:

$$\phi_{s.w.}(x) = \sqrt{\frac{2}{a}} sin(k_n x)\theta(a - x)\theta(x) \tag{19}$$

up to the $2/a$ normalization factor, the Wigner transform is again given by eq. (16) with two differences: i)only the discrete values of $k$ are allowed :$k_n = n\pi/a$, ii)eq. (16) holds only for $q < a/2$, for $q > a/2$ one has to complete by symmetry around $q = a/2$; hence it is a closest wall that determines the behaviour in $p$-space. Indeed to derived the desired result, withouth lengthy calculation it is sufficient to start from the one wall model, put the mirror at $q = a/2$ and keep only the wavefunctions which are left unchanged by the

mirror symmetry. The resulting Wigner transform is plotted in Fig. 2a for the n=3 orbit. Note that the height of the peak ( for $q < a/2$ ) is given by eq. (18) but for $p = \hbar\pi n/a$, i.e. $f_{r,max} = \frac{2q}{a}(1 - j_0(\frac{4q\pi n}{a}))$, so that its linear behaviour is modulated by the Bessel function, as can be seen on the figure.

The next step towards a more realistic potential is to replace the infinite walls by soft ones. The resulting Wigner transforms are not analytic any more, but their new features can be again understood using semiclassical and classical concepts. In the WKB method it is assumed that when the variation of the potential is slow, the wavefunction of the n-th orbital can be locally approximated by a plane wave so that to each point ,$x$ , one can associate a local momentum , $p(x)$, given by

$$p_n(x) = \pm\sqrt{2m(E_n - V(x))} \tag{20}$$

where $E_n$ is the eigenenergy of the level. For the square well this prescription gives the two momenta , $\pm\hbar n\pi/a$, as expected.

Next we consider a potential with the surface more diffuse, as the case of the stretched harmonic oscillator defined in ref.[9] as:

$$V(x) = \begin{cases} 0, & \text{if } 0 < x < a; \\ \frac{1}{2}m\omega^2(x-a)^2, & \text{if } x > a \end{cases} \tag{21}$$

and symmetric for negative x. Note that this potential has two well known limiting cases: the infinite square well ($\omega \to \infty$) and the harmonic oscillator ($a \to 0$). In Fig. 2b we show the Wigner transform for the n=8 orbit of the SHO potential. In this case, $a/b_{ho} \gg 1$ ($b_{ho} = \sqrt{\frac{\hbar}{m\omega}}$), and the SHO potential can be well approximated by the infinite square well with the same a. As it is expected the two Wigner transform are very similar, and the most important features of Fig 2b can be understood from (16). Nevertheless some changes appear due to the surface diffuseness: i) due to the added attraction, the energies, $E_n$, are lower than those of the infinite square well, and this decreases the local momentum for all $x$, ii) the wavefunction does not vanish when $|x| > a$, and at these large values of $x$ one expects from (20) to find $k_n$'s decreasing towards zero at the classical turning points. These

features can be seen in Fig. 2b. Varying the values of $\hbar\omega$ in (21) the role of the surface diffuseness can be very easily studied in this model. As it is shown in [ref. 10] the bumps of the Wigner transform are more pronounced for small values of the surface diffuseness. The position of the maximum value coincides with the prediction of the local momentum (20) only for $a/b_{ho} \gg 1$. When $a/b_{ho} \to 0$ $(SHO \to HO)$ the position of the quantal maxima is shifted with respect to the semiclassical prediction (20). As shown by Berry [11] this general feature of the Wigner transform can be understood using the WKB approach for $f(q,p)$. In this approach $f(q,p)$ is given by the Airy function. In the case of the HO potential and for the values of $p$ and $q$ near of the classical trajectory $\frac{h_0}{4} = \frac{p^2}{2m\omega\hbar} + \frac{m\omega q^2}{2\hbar} = n + 1/2$, the Wigner transform reads:

$$f_{WKB}(p,q) = \frac{2^{2/3}}{(n+1/2)^{1/3}} Ai[(h_0/2 - (2n+1))(2n+1)^{-1/3}] \tag{22}$$

Note that the classical trajectory does not correspond to the maximum of the Airy function which its not reached for the argument equal to zero (corresponding to the classical trajectory) but for the argument equal to -1. One can recover the classical trajectory in the limit $\hbar = 0$, using the property:

$$\lim_{\hbar \to 0} \frac{1}{\hbar} Ai(\frac{x}{\hbar}) = \delta(x) \tag{23}$$

and this delta function is peaked for values of p and q given by eq. (20).

As an illustration we have calculated the exact [6] and WKB Wigner transforms for the $6^{th}$ level of the H.O. potential (see fig. 3), the classical trajectory corresponds to $h_0 = 22$, near this value $f_{WKB}(p,q)$ is a very accurate approximation to the quantal result. As it is shown in Table I the position of the outer quantal maximum is fairly well reproduced by the WKB approach even for small values of n.

b) **N particles**

In fig. (4) we show the Wigner Transform for N occupied levels for the infinite square well potential. From eq (6) it is clear that for a Slater determinant each orbital contributes additively to the total Wigner Transform. It can be checked that each of the sucessive

valleys and ridges in $f(q,p)$ as one goes from the center ($q=0, p=0$) to the surface is due to the filling of a new orbit.

In order to get insight into the N fermions problem, let us study the infinite and the semi-infinite system case. In the infinite system $f$ is $q$-independent and given by

$$f(q,p) = \theta(k_F - \mid \frac{p}{\hbar} \mid) \tag{24}$$

where $k_F = \pi\rho$ is the Fermi momentum ($\rho = \lim_{N\to\infty a\to\infty} \frac{N}{a}$). The limiting case of the half infinite system can be found starting from the Wigner transform for the infinite square well . Adding over infinite levels, taking $a \to \infty$ with $\rho$ constant, we find from eq. (16)

$$f(q,p) = \int_{2q(\frac{p}{\hbar}-k_F)}^{2q(\frac{p}{\hbar}+k_F)} \frac{sint}{t} dt - \frac{1}{2} j_0(\frac{2pq}{\hbar}) sin(2k_F q) \tag{25}$$

Eq. (25) is plotted in fig. 5. The similarity between figs. 4 and 5 suggests that some semiclassical approaches developped for the half infinite systems [12] can be useful also for one dimensional finite systems. As already noticed by Ayachi et al. [13] the oscillations at $p=0$ remain with period $\pi/k_F$ and are not damped even far away from the wall. In the limiting case $qk_F >> 1$ we can understand this behaviour analytically. Starting from (25) we find:

$$f(q,p) = \theta(k_F - \mid \frac{p}{\hbar} \mid) - 2\delta(\frac{p}{\hbar}) sink_F q \tag{26}$$

The first term of this expression is just that of the infinite matter and the second term is responsible for the oscillatory behaviour at $p=0$.

## IV. Concluding Remarks

It is possible to understand the gross features of the Wigner transform using the square well potential and semiclassical models . If the potential is approximately constant over a long range (system with saturation) the square well potential allows to understand analytically the most important features of the Wigner transform. In the other cases the most important features can be understood making the WKB approximation, and the classical trajectory

is only recovered for $\hbar = 0$. The half infinite limit can be reached adding over infinite shells with the constraint $\rho =$ constant, and in this case the oscillations at $p = 0$ remain.

This work has been financed by grants from DGICYT (PB-87-0311 and PS-88-0045) and by the exchange programs between the French and Spanish governments.

# References


[1] E. Wigner, Phys. Rev. **40** (1932)749

[2] H. Weyl, Z. Phys. **46** (1927)1 E.C. Kemble "Fundamental Principles of Quantum Mechanics" Mc Graw Hill (N. Y.) (1937) pag. 90-122

[3] J.G. Kirkwood, Phys. Rev. **44** (1933)31

[4] P. Carruthers and F. Zachariasen, Rev. Mod. Phys. **55** (1983)245

[5] J. Perina, "Quantum Statistics of Linear and Non Linear Optical Phenomena" Reidel (1984) 81.

[6] S. Shlomo and M. Prakash, Nucl. Phys. **A357** (1981)157

[7] J. Martorell and E. Moya, Ann. Phys.**158** (1984)1

[8] A. Bohr and B.R. Mottelson "Nuclear Structure" Vol.I Benjamin (1969) 223

[9] M. Casas, H. Krivine and J. Martorell, Am. J. Phys. **57** (1989)35

[10] M. Casas, J. Martorell and H. Krivine, Ann. Fis. **A83** (Spain )(1987)122

[11] M.V. Berry, Phil. Trans. Roy. Soc. **287** (1977)237

[12] N. L. Balazs and G.G. Zipfel Jr., Ann. Phys. **77** (1973)139

[13] Ayachi et al., Z. Phys. **A327**(1987)141

[14] L. Cohen, Proc. of the IEEE **77**(1989) $n^0$ 7

[15] G.A. Baker, I.E. Mc Carthy and C.E. Porter, Phys. Rev. **120** (1960)254

## Figure Captions

Fig. 1 Quantal Wigner Transform for $^{40}Ca$ obtained with the Woods Saxon potential . For comparison we also show the prediction of the Thomas Fermi model. $V_0 = -55MeV$, $R_0 = 1.2A^{1/3}fm$ and $a_0 = .50fm$.

Fig. 2 a) Wigner Transform for the $8^{th}$ level of the infinite square well potential ($a = 8.5fm$). b)For comparison we also show $f(q,p)$ for the same level of the SHO well with the same value of $a$.

Fig. 3 Comparison between the quantal (solid line) and the WKB (dotted line) Wigner Transforms as a function of $h_0$ for the $6^{th}$ level of the H.O. potential.

Fig. 4 $f(q,p)$ for 8 occupied levels of the infinite square well potential (the value of $a$ is the same of Fig. 2).

Fig. 5 Wigner Function truncated at q= 12 fm of the half infinite potential for $k_F = 1.12fm^{-1}$.

## Table Caption

Table 1 Values of $h_0$ corresponding to the maxima of the Wigner transform given by the WKB and quantal prescription for the first five levels of the H.O.. For comparison the position of the classical trajectory is shown in the third column.

TABLE I

| n | Quantal | WKB | Classical |
|---|---|---|---|
| 0 | 0 | 0 | 2 |
| 1 | 3 | 3,12 | 6 |
| 2 | 6,45 | 6,58 | 10 |
| 3 | 10,04 | 10,17 | 14 |
| 4 | 13,70 | 13,84 | 18 |
| 5 | 17,41 | 17,55 | 22 |

Fig. 1

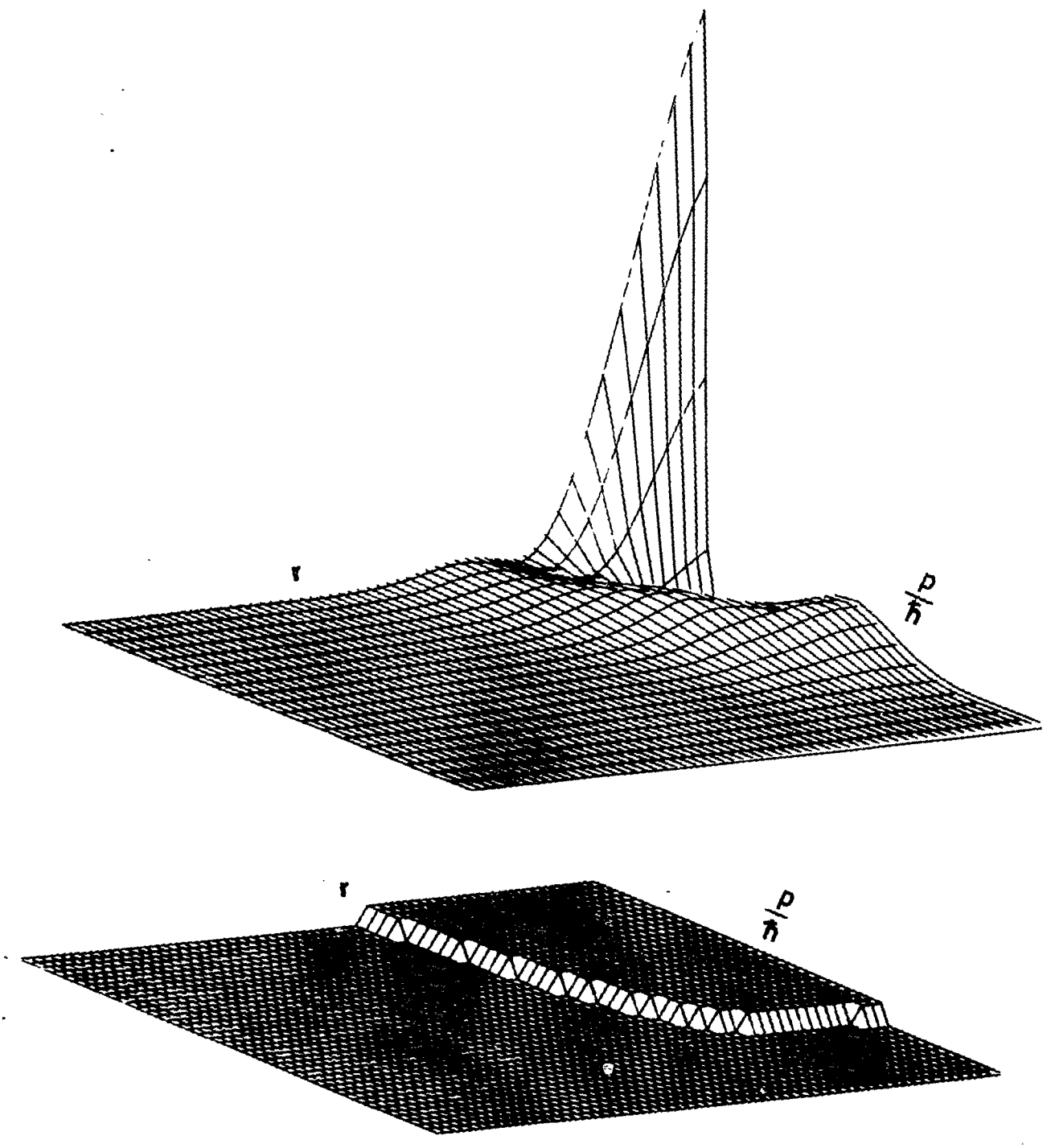


r [0,12] [fm]
p/ħ [0,2] [fm-1]

Fig. 2a

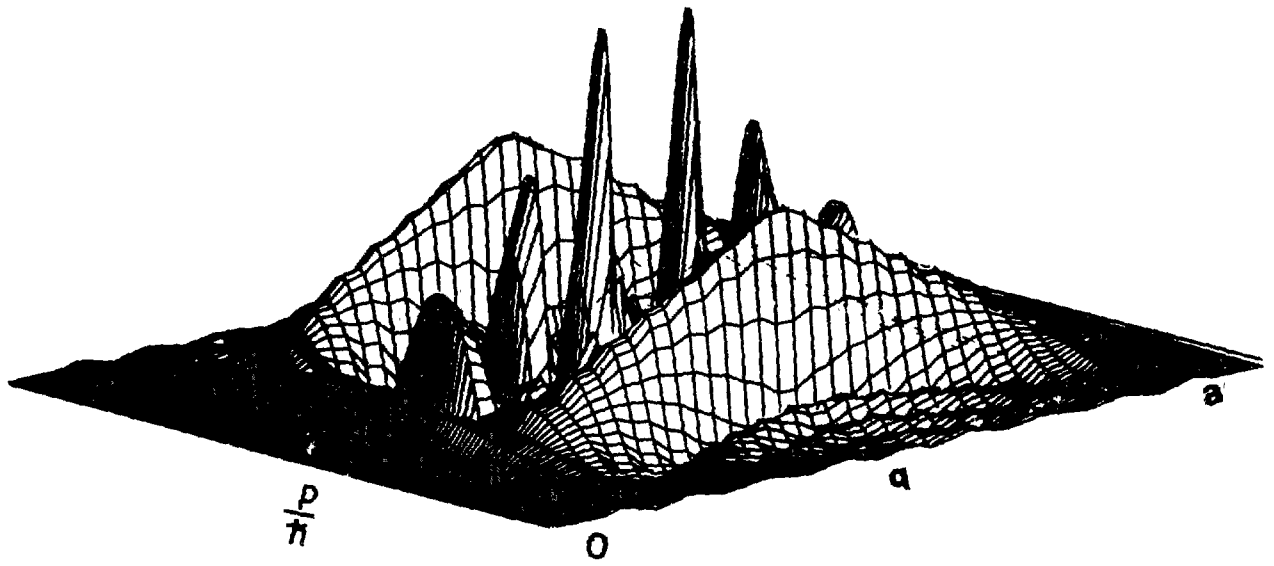


$\frac{p}{\hbar}$ [-3, 3]

Fig.2b

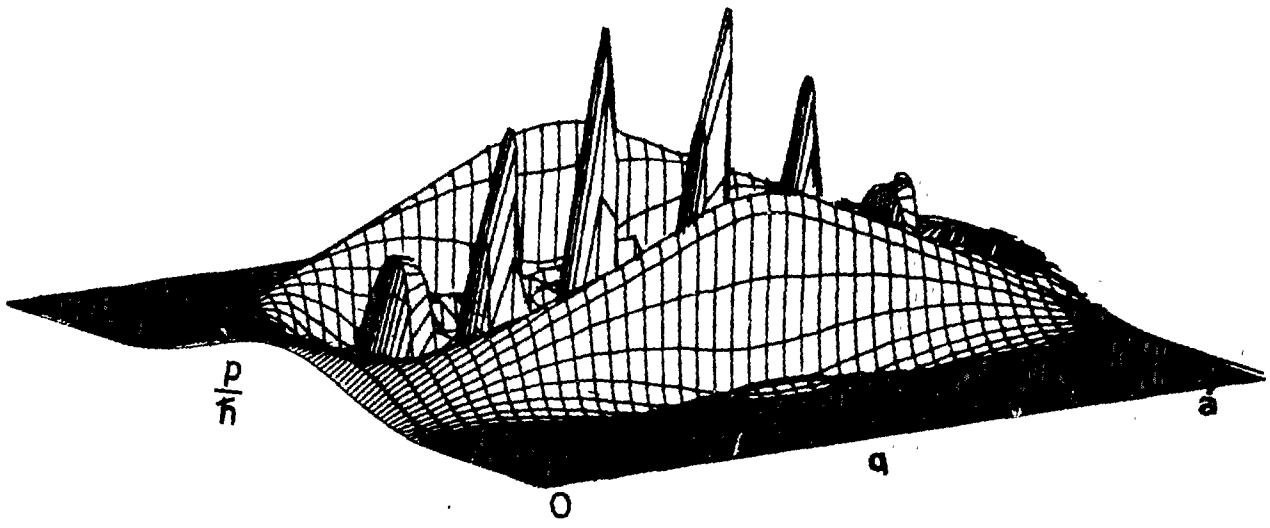


$\frac{p}{\hbar}$ [-3,3]

Fig. 3

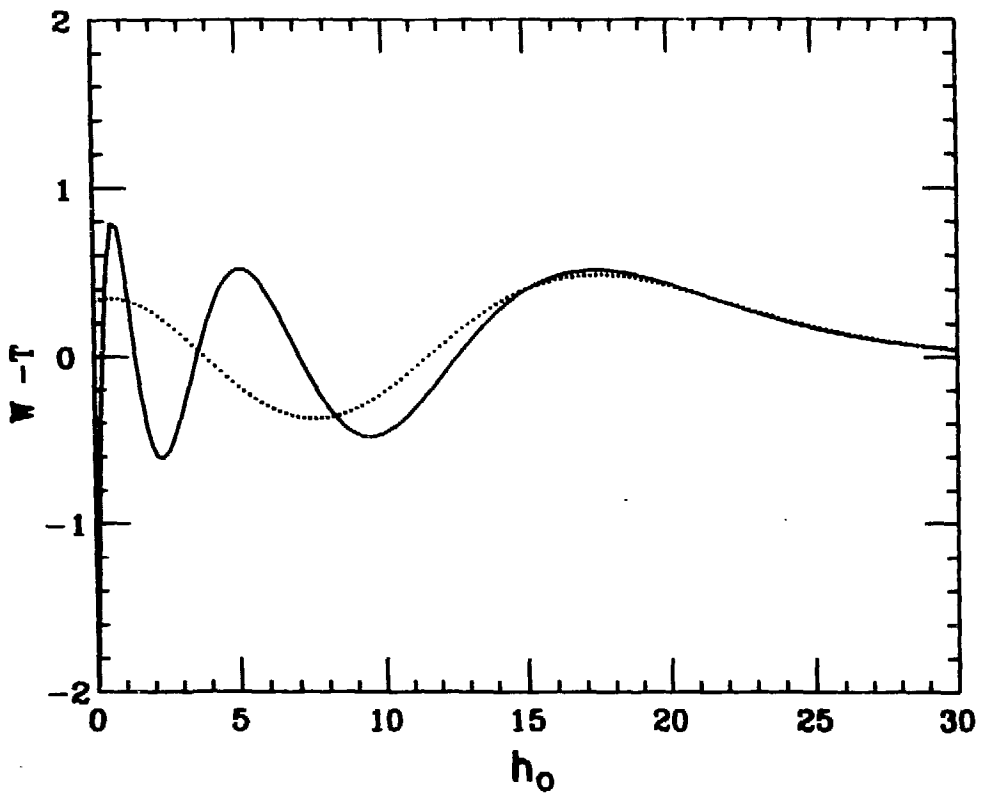

Fig. 4

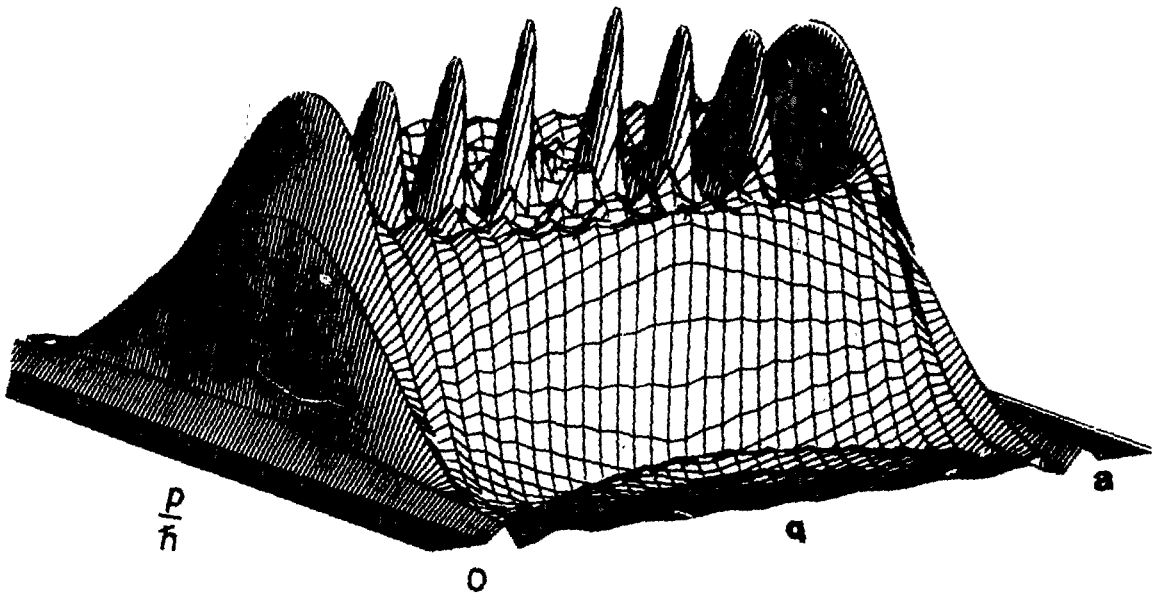

Fig. 5